Transport in Intermediate and High Molecular Weight Hydroxypropylcellulose/Water Solutions†

George D. J. Phillies,* Carla Richardson, and Carol Ann Quinlan

Department of Physics, Worcester Polytechnic Institute, Worcester, Massachusetts 01609

S. Z. Ren

Department of Physics, University of South Dakota, Vermillion, South Dakota 57069

Received May 4, 1993; Revised Manuscript Received September 24, 1993®

ABSTRACT: We obtained the shear viscosity η and optical probe (67-nm polystyrene latex spheres) diffusion coefficient D in hydroxypropylcellulose (HPC)/water at temperatures $T = 10, 25$, and 39 °C. Polymer samples had weight-average molar masses M of 139, 146, 415, and 1280 kDa. Polymer concentrations c ranged up to 40–100 g/L; η was as large as 10^3–10^6 cP in different systems. η has a stretched-experimental dependence on c at small c and power-law behavior at large c. D generally follows a stretched exponential $D_0 \exp(-\alpha c^\nu)$ but is consistent with power-law behavior at large c. Individual spectra fit well to Williams–Watts forms $A_0 \exp(-\theta t^\beta)$. The dependence of α, ν, θ, and β on c, M, and T is discussed.

Introduction

The nature of polymer dynamics in dilute and concentrated solutions is a significant topic of current research. Some researchers use the de Gennes[1]–Doi–Edwards[2] models of polymer solution dynamics, though other models are also extant.[3-9] Recent evaluations of these models include Lodge et al.'s,[10] who conclude "it is unlikely that reptation is significant in the semidilute regime", and Skolnick and Kolinski,[11] who observe "...the matter is not at all settled in favor of reptation in a fixed tube, and an abundance of evidence argues against the simple reptation model's validity".

This paper is concerned with physical solution properties, namely, viscosity and optical probe diffusion, of hydroxypropylcellulose (HPC), a nonionic, semirigid, chemically-modified biopolymer soluble in water over a wide range of concentrations. The programmatic objective here is to test modern dynamic models[1-9] and to ascertain the importance of effects unique to specific polymers. Previous studies of HPC/water using probe diffusion include Yang et al.,[12] Brown et al.,[13] Russo et al.,[14-16] and this laboratory.[17] Our study is novel in that we worked to far larger polymer concentrations at several temperatures and found simple nonexponential forms that fit our spectra well.

In optical probe diffusion[18] experiments, one observes the diffusion of mesoscopic probe particles through a polymeric background and infers the polymer dynamics from the probe motion. The method may be traced back to light scattering experiments of Turner and Hallet[19] and ultracentrifuge studies of Laurent and Pietruszkiewicz.[20] This laboratory has reported studies on aqueous solutions of neutral polymers[21,22] and nonneutralized[23] and neutralized[24] polyelectrolytes.

Theoretical interest in optical probe diffusion includes de Gennes' note[1] that such measurements, made with probes of differing radius, could determine the mesh size ξ of the hypothesized pseudogel lattice of semidilute polymer solutions. Interest in this technique in other laboratories arose from an interest in modeling biological fluids[19] and from the observation that the Stokes–Einstein equation

$$D = \frac{k_B T}{6\pi\eta R} \tag{1}$$

(where k_B is Boltzmann's constant, T is the absolute temperature, η is the solution viscosity, and R is the probe radius) fails badly[23] for mesoscopic (R up to 0.3 μm) probe particles in solutions of some though not all high-molecular-weight polymers.

Inspired by a suggestion of Langevin and Rondelez,[25] in many[18] but not all[22] systems D is found to depend on concentration via

$$D = D_0 \exp(-\alpha c^\nu) \tag{2}$$

where D_0 is D in the absence of polymer, c is the polymer concentration, and α and ν are scaling parameters. Contrary to some model-based expectations,[25] α depends strongly on polymer molecular weight M, with $\alpha \sim M^{0.9\pm0.1}$ being found over a wide range of M. For mesoscopic (>20 nm) probes, α is nearly independent of probe radius R; recent work of Russo shows that α depends on R for smaller probes.[14] Phillies and Peczak[26] found that the corresponding

$$\eta = \eta_0 \exp(\alpha c^\nu M^\gamma) \tag{3}$$

empirically describes polymer viscosity up to very large polymer M and c.

A paradox arises if eqs 2 and 3 are extrapolated to arbitrarily large c and M. In polymer melts, D and η appear to follow scaling laws, e.g.

$$\eta = \bar{\eta} c^x M^y \tag{4}$$

with x and y scaling exponents and $\bar{\eta}$ a prefactor. If one extends eqs 2–4 to large M, the predicted solution viscosity exceeds the predicted melt viscosity, contrary to any expectation that solvents are plasticizers.

In a recent paper,[28] this paradox was resolved, demonstrating from the literature (for full references, see ref 28) that at sufficiently large η one observes at least in some systems a transition from low-c stretched-exponential ("solutionlike") behavior to large-c scaling-law ("meltlike") behavior. Such transitions are typically only evident for $M > 1 \times 10^6$ and $\eta/\eta_0 > 10^3$. At smaller M and η only solutionlike (stretched-exponential) behavior is seen.

* To whom communications may be addressed. EMail: phillies@wpi.wpi.edu (Internet).

† The partial support of this work by the National Science Foundation under Grant DMR91-15639 is gratefully acknowledged.

® Abstract published in *Advance ACS Abstracts*, November 1, 1993.

0024-9297/93/2226-6849$04.00/0

Table I. Molecular Weight Distributions of Hydroxypropylcellulose Samples (All Molar Masses in kDa)

nominal M	M_n	M_w	M_w/M_n
60	93	139	1.50
100	100	146	1.45
300	191	415	2.17
1000	1120	1280	1.15

The following section of the paper discusses our experimental methods. Further sections treat solution viscosity, probe diffusion coefficients, and spectral line shapes. Comparison with previous studies of probe diffusion in HPC/water[12-16] shows reasonable agreement at all points at which comparison can be made. A discussion and summary close the paper.

Experimental Methods

We studied water/hydroxypropylcellulose (HPC); samples had *nominal* molar masses of 60, 100, 300, and 1000 kDa (Scientific Polymer Products, Ontario NY, lots 1, 3, 2, and 1, respectively). The solvent was conductivity water (>14 MΩ) prepared by reverse osmosis and ion exchange (Milli-RO, Milli-Q; Millipore, Inc.) units. Probe particles were carboxylate-modified polystyrene latex spheres with 67-nm nominal diameter (Polysciences, Inc.). To prevent polymer adsorption by the spheres, most solutions contained 0.1 or 0.2 wt % Triton X-100 (Rohm & Haas; Aldrich, Milwaukee, WI).

Full polymer molecular weight distributions were determined[32] with aqueous size-exclusion chromatography, based on a Waters Associates M6000A solvent delivery system, U6K sample injector, and a TosoHaro G5000PW$_{XL}$ column using 0.5 M NaOH as eluent. An R401 differential refractometer and an on-line LDC/Milton-Roy KMX-6 low-angle laser light scattering system were detectors, determining the concentration and weight-average molecular weight $(M_w)_v$ of each elution volume. Refractive index increments are determined internally; we did not rely on literature values of $\partial n/\partial c$. Integration of the $(M_w)_v$ curve gives conventional number- and weight-average molar masses M_n and M_w (Table I).[32] The 60, 100, 300, and 1000 kDa HPC had measured M_w values of 139, 146, 415, and 1280 kDa, respectively. The 60, 100, and 300 kDa HPC were commercial materials having broad molecular weight distributions; the 1 MDa HPC had a measured M_w/M_n of 1.15. At very large M, mixing artifacts can enhance the apparent M_n, reducing the apparent polydispersity but not affecting M_w significantly; it is difficult to assess the importance of this effect.

Viscosities were measured with Cannon-Fenske and Ubbelohde viscometers mounted in a stirred water bath. To avoid kinetic energy corrections, flow times were systematically kept above 240 s. The bath temperature was regulated to within 0.1 °C. Solution densities were determined using conventional volumetric glassware. Some samples were studied with several sizes of viscometer, flow times varying typically by 5-fold. η was nearly independent of flow time; no signs of shear thinning are apparent in our data.

Probe diffusion coefficients were measured with quasi-elastic light scattering spectroscopy. Sample cells were square glass or polystyrene fluorimeter cuvettes, four sides polished, precleaned by rinsing the cells repeatedly with dust-free (0.2-μm filter) water, and dried with dry dust-free (0.1-μm filter) nitrogen. Samples were prepared from stock solutions by serial dilution and filtration through 0.2-μm microporous filters into clean sample cells, into which a trace of probe spheres was added. Light sources were a He–Ne laser (6328 Å, 35 mW) and an Ar$^+$ laser (5145 Å, 1.5 W maximum power). With the He–Ne laser, light scattered through 90° was isolated by a pair of irises and detected with an RCA 7265 photomultiplier tube; photopulses were sent to a Langley-Ford Instruments 144-channel (128 linearly spaced data channels; 16 base-line channels placed after a 1024-channel digital correlator. The Ar$^+$ laser was used in conjunction with a Brookhaven Instruments goniometer and 2030AT 270-channel (264 data channels, 6 base-line channels) correlator for angular dependence and contrast studies. Detector count rates were typically 150 000 counts/s; integration times were at least 300–600 s. The sample temperature in the He–Ne apparatus was stabilized by mounting the cells in a massive copper block through which temperature-stabilized water was passed; the nominal bath stability is 0.1 °C.

Table II. Viscosity of Low-Concentration Hydroxypropylcellulose/Water Solutions as Fit to $\eta = k_0 + k_1c + k_2c^2$, Intrinsic Viscosities, and Critical Overlap Concentrations c^*

M	T	k_0	k_1	k_2	$[\eta]$	c^* (g/L)
60	10	1.302	0.181		0.139	7.19
	39	0.670	0.073		0.109	9.18
100	10	1.30	0.262		0.202	4.96
	39	0.666	0.101		0.152	6.59
300	10	1.305	0.663	0.162	0.508	1.97
	39	0.668	0.239	0.054	0.358	2.79
1000	10	1.325	1.561	1.595	1.18	0.85
	39	0.691	0.352	0.672	0.509	1.96

In most experiments, the correlator sample time (channel width) was set so that the $^1/_2$-decay point of the spectrum was found between the 15th and 30th channels. We required that the measured long-time base line agrees with the theoretical P^2/N base line (where P is the total number of photocounts and N is the experiment's duration in sample times) to within the postdetection signal-to-noise ratio. In a few experiments, multiple spectra were obtained of the same sample using geometrically spaced channel widths.

Koppel's method of cumulants[30,31] was used to analyze all individual spectra. In this method, spectra $S(k,t)$ are reduced to field correlation functions $g^{(1)}(t)$ and fit to

$$\ln [g^{(1)}(t)] \equiv 0.5 \ln[S(k,t) - B] = \sum_{l=0}^{N} \frac{K_l(-t)^l}{l!} \qquad (5)$$

Here B is the base line, the K_l are cumulants, and N is the fit order—the truncation level. K_1 gives a diffusion coefficient via $D = K_1q^{-2}$, q being the magnitude of the scattering vector. Fits were made with $N \in 1, ..., 4$, the optimum N being the smallest value that represents the data to within the intrinsic signal-to-noise ratio of the experiment. Use of fits with large-than-optimum N does not significantly improve the root-mean-square difference between the fitting function and the data. We also employed nonlinear least-squares fitting procedures described below.

The signal-to-noise ratio S/N is the ratio of $S(k,0)$ to the root-mean-square difference between $S(k,t)$ and the fitting function. Experimental signal-to-noise levels S/N are determined by two factors. First, the postdetection signal-to-noise ratio is limited by photon counting statistics, so that S/N cannot be better than $\approx S(k,t)^{1/2}$ (where $S(k,t)$ includes B, so $S(k,t) \gg 0$ at $t \to \infty$). Second, the predetection signal-to-noise ratio is limited by the sampling of the underlying physical process. With infinite scattered light intensity S/N cannot be better than $\approx(\Gamma T)^{1/2}$, where $\Gamma \approx K_1$ is the relaxation rate of the underlying random process and T is the integration time. For our experiments, photocount rates generally exceeded 30 photons per correlation time Γ^{-1}, while the experimental integration time was 5–10 min, giving a typical ΓT of order 10^6 and a typical $S(k,t) \gg \Gamma T$. Under these conditions, the predetection signal-to-noise ratio limits the experimental S/N; an S/N of 500–1000 would typically be expected under our conditions. Observed S/N were slightly worse than this, typically ≈300–500.

Solution Viscosities

Low-concentration viscosity measurements determine the intrinsic viscosity $[\eta]$ and critical overlap concentration $c^* = 1/[\eta]$ of each system. Determinations were made at 10 (near-good solvent), 25, and 39 °C (Θ-like solvent). The data follow (Table II)

$$\eta = k_0 + k_1c + k_2c^2 \qquad (6)$$

the k_i being fitting parameters, where $[\eta] = k_1/k_0$. For 60 and 100 kDa HPC, η is linear in c (i.e., $k_2 \approx 0$); for 300 kDa and 1 MDa HPC, η is manifestly quadratic in c.

Viscosity measurements were also made to large c (0–100 g/L for 60, 100, and 300 kDa HPC; 0–40 g/L for 1 MDa HPC). For 300 kDa and 1 MDa HPC, viscosities as large as 10^6 cP were encountered. Unlike most systems studied

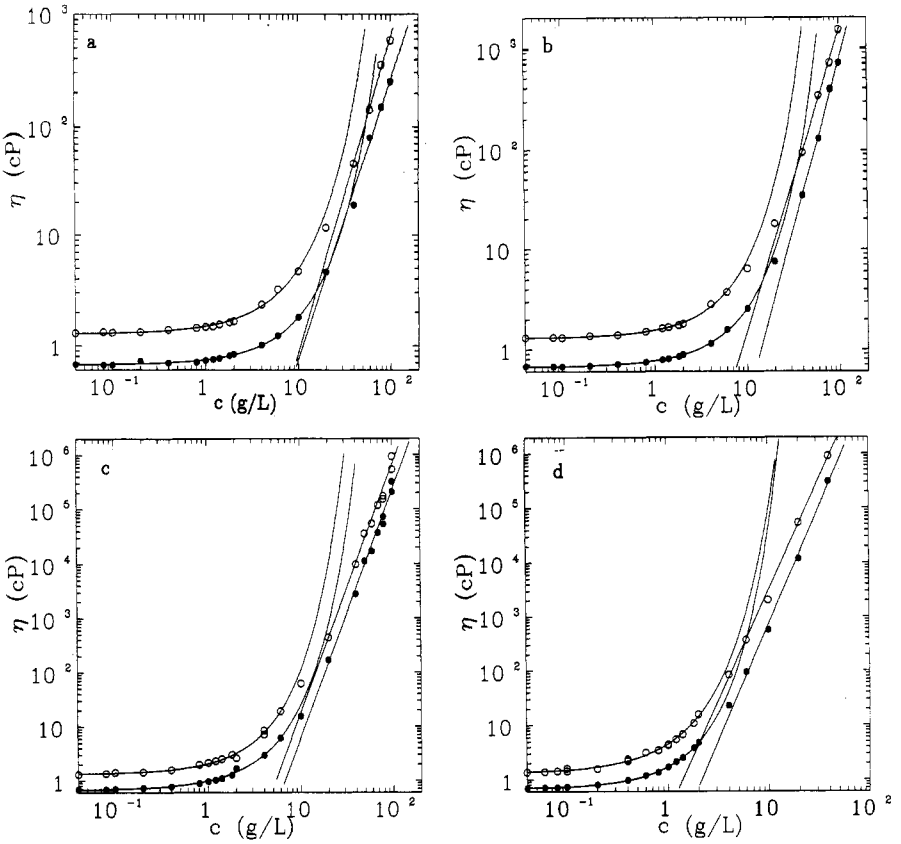

Figure 1. Solution viscosities of hydroxypropylcellulose/water for nominal HPC molar masses of (a) 60, (b) 100, (c) 300, and (d) 1000 kDa at 10 (open circles) and 39 °C (filled circles). Smooth curves are fits to $\eta_0 \exp(-\alpha c^{\nu})$, while straight lines are fits to $\bar{\eta}c^{x}$.

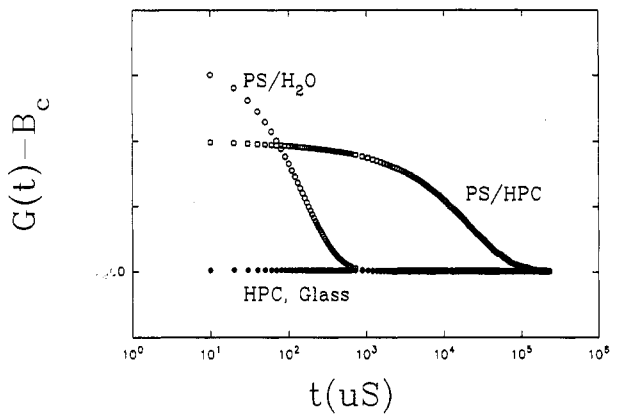

Figure 2. Spectra of polystyrene spheres in water (PS/H_2O) and in 40 g/L of 300 kDa HPC (PS/HPC) which dominate spectra of sphere-free 40 g/L of 300 kDa HPC (HPC) or of a local oscillator (Glass), which has no detectable time dependence.

previously by this laboratory, in HPC/water η does not simply follow a stretched exponential in c. An accurate description of η is obtained by describing the lower-c regime with solutionlike (stretched-exponential) behavior and the higher-c regime with meltlike (power-law) behavior (Figure 1 and Table III). Smooth curves mark fits to eq 3 (including the $c = 0$ datum), while straight lines are fits to a power law

$$\eta = \bar{\eta}c^{x} \tag{7}$$

Tube-type theories of polymer dynamics predict x is 3 for rods and 3.5–3.75 for chains under Θ or good conditions.[2] Pearson[27] argues for $x = 4.25$ for semidilute chains in good solvents, in good agreement with the $x = 4.3 \pm 0.3$ found in our data. Figure 1 is consistent with other polymer systems (albeit primarily synthetic organophilic polymers have c and M larger than those seen here), where the same solution-to-melt transition has previously been noted.[28] However, here the transition occurs at $\eta \approx 100$ cP, much lower than the transition viscosity $\sim 10^4$ cP observed[28] in other solutions. In particular, schizophyllan solutions[29] show no such transition for $\eta \leq 10^4$ cP. Since schizophyllans are rigid, have a large-c ordered phase, but do not have a low transition viscosity, the low transition viscosity of our solutions appears not to arise from chain rigidity or nearness to a liquid–liquid crystal phase transition in HPC/water.

Table III. Viscosity of Hydroxypropylcellulse/Water Solutions, as Fit to $\eta = \eta_0 (\exp(\alpha c^{\nu})$ and $\eta = \bar{\eta}c^{x}$, and Root-Mean-Square (rms) Fractional Errors and Cut-Off Concentrations in the Fits

M (kDa)	T	c_M (g/L)	η_0	α	ν	% rms	c_m (g/L)	$\bar{\eta}$	x	% rms
60	10	10	1.12	0.160	0.93	3.4	40	1.2×10^{-3}	2.9	5.8
	39	20	0.67	0.109	0.96	2.0	20	2.2×10^{-3}	2.5	15
100	10	6	1.30	0.182	0.99	2.0	40	1.6×10^{-3}	3.0	5
	39	10	0.66	0.145	0.97	1.4	40	1.34×10^{-4}	3.4	7
300	10	6	1.32	0.443	1.00	6.5	20	4.98×10^{-4}	4.6	26
	39	6	0.66	0.406	0.95	4.9	20	1.75×10^{-4}	4.6	25
1000	0	2	1.31	1.23	0.96	6.0	4	0.26	4.06	18
	39	2	0.68	0.92	1.08	1.7	6	3.85×10^{-2}	4.3	19

Fitting parameters are partly determined by the choice of boundary between solutionlike and meltlike regimes. Table III reports boundaries taken from the root-mean-square fraction error R to each fit. Equation 3 was fit to data extending from pure solvent up to a cut-off concentration. There is a maximum concentration c_M below which η follows eq 3 to within a few percent. If c is increased above c_M, R increases markedly. Similarly, there is a minimum concentration c_m below which η ceases to follow eq 7 accurately. Table III reports best values of c_M and c_m.

Validation of Probe Results

The objective of an optical probe study is to examine probe diffusion in a matrix (background) solution; a probe

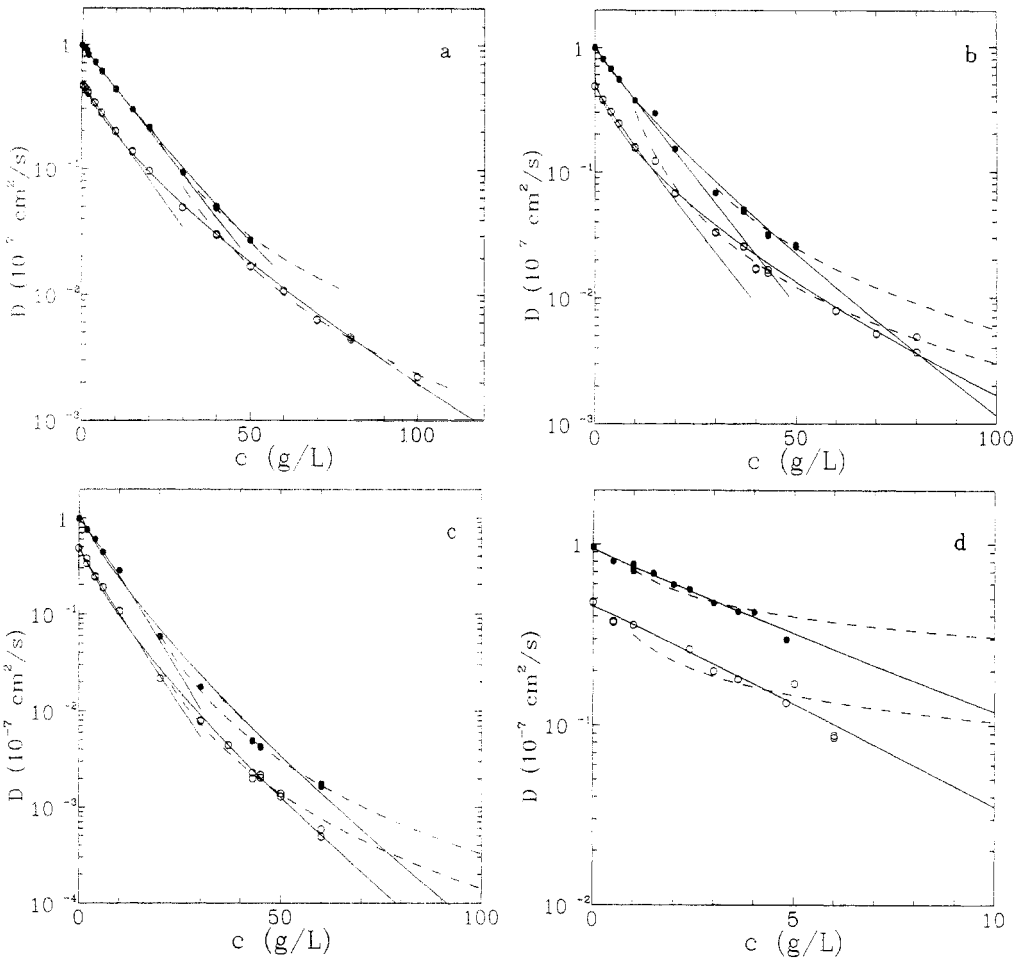

Figure 3. Probe diffusion coefficient of 67-nm polystyrene latex spheres in HPC/water at temperatures of 10 (open circles) and 39 °C (filled circles) for (a) 60 kDa, (b) 100 kDa, (c) 300 kDa, and (d) 1 MDa HPC. Solid lines are stretched exponentials, dashed lines are power laws.

Table IV. Probe Diffusion Coefficients in Hydroxypropylcellulose/Water Solutions, as Fit to (i) $D_0 \exp(-\alpha c^{\nu})$ and (ii) $D_0' \exp(-\alpha' c^{\nu'})$ for $c < c_M$ and $\tilde{D}c^{-x}$ for $c > c_m$, c_M and c_m Being from Table III

M (kDa)	T	D_0	α	ν	% rms	D_0'	α'	ν'	% rms	$\tilde{D}$	x	% rms
60	10	0.55	0.20	0.72	6.2	0.49	0.096	0.97	1.2	1150	2.85	4.4
	39	1.03	0.11	0.90	3.1	1.00	0.086	0.98	1.5	169	2.21	4.9
100	10	0.60	0.37	0.63	13	0.48	0.13	0.93	0.5	31.6	2.01	9.5
	39	1.06	0.15	0.82	10.2	0.99	0.101	0.98	0.5	116	2.16	5.8
300	10	0.57	0.31	0.76	11.5	0.49	0.175	0.95	4.0	517	3.28	16.7
	25	0.83	0.29	0.78	20	0.71	0.138	1.09	10	2567	3.67	19
	39	1.25	0.28	0.78	19	0.99	0.117	1.07	1.6	1007	3.24	4.0
1000	10					0.45	0.23	1.04	12	0.32	0.48	21
	39					0.95	0.24	0.94	4.3	0.72	0.37	10

diffusion coefficient D often suffices to characterize this motion. A variety of artifacts can interfere with such measurements. Matrix-induced probe aggregation and adsorption of the matrix polymer by the probe may cause the probe radius to depend on matrix concentration, obscuring further data interpretation. Furthermore, light scattering is nonselective. Spectra of matrix/probe mixtures contain components due to matrix scattering, so the apparent D potentially reflects matrix as well as probe motions.

To prevent polymer adsorption and polymer-induced probe aggregation, traces of Triton X-100 were added to all solutions. A suitable surfactant concentration c_T was determined by measuring D against c_T at fixed c, c being in the upper ranges that we used. In each system studied and at both temperatures, D is very small at low c_T (≤0.01 vol %). At larger c_T, D rises swiftly to a plateau. This combination of behaviors indicates competitive binding of surfactant and matrix polymer to the probes. At low c_T the probes adsorb polymer chains, aggregate, and diffuse slowly. At larger c_T, the surfactant displaces the polymer; D of individual spheres is seen. Surfactant binding is saturating, increases in c_T above the plateau value not affecting D.

For all M and both temperatures, D attains its plateau at a c_T below 0.1 vol %. We used c_T = 0.1 vol % in the 60, 100, and 300 kDa polymer solutions, and c_T = 0.2 vol % with 1 MDa HPC. Our earlier study[17] on 60 kDa HPC used 0.01 vol % Triton X-100; present results are consistent with ref 17. The surfactant can also affect D directly by changing hydrodynamic properties of the solution,[33] but only for c_T well above values used here.

Multiple scattering by the polystyrene probes is not significant. Multiple scattering is revealed by a dependence of D on sphere concentration c_s. We used a fixed polystyrene latex concentration < 0.1 vol %, which is well below the c_s at which D of spheres in pure water depends on c_s. Adding HPC reduces the index-of-refraction mismatch between spheres and solution, so in solution multiple scattering effects are even weaker than in pure water, where they are not significant.

To test for matrix scattering, we studied probe/matrix/solvent and matrix/solvent mixtures under identical conditions (laser power, iris settings, correlator channel widths, integration time). The elevated osmotic compressibility of concentrated polymer solutions depresses scattering from these solutions; we examined both small and large c. Typical results appear in Figure 2, which shows background-subtracted intensity correlation functions for probes in water, probes in 40 g/L of 300 kDa HPC, and the same HPC solution with no added probes.

The HPC spectrum is far weaker than spectra of probe-containing solutions. Transforming to the field correlation function $g^{(1)}(k,\tau) = [S(k,\tau) - B]^{1/2}$ and rescaling shows that we obtain clean spectra of HPC in water, but $g^{(1)}(k,\tau)$ for plain HPC is only a few percent of $g^{(1)}(k,\tau)$ of probe/matrix systems. Matrix scattering thus is not important here.

Our interpretation of probe spectra is based on theoretical analyses of nondilute three-component systems.[34,35] To summarize the theory, the light scattering spectrum of a three-component probe/matrix/solvent system is expected to contain two (exponential, in the mean-field linear-response limit) relaxations. If both macrocomponents are dilute, the relaxations are assignable one-to-one to individual macrocomponents. If the solution is nondilute, in general, there are still two relaxational modes, but the modes can no longer be assigned to single components. If both macrocomponents are nondilute and if one species dominates the scattering intensity while the other species scatters no light at all, both relaxational modes still appear in $g^{(1)}(k\tau)$. However, as shown 2 decades ago,[34,35] if only one (probe) species scatters light *and if the probes are dilute*, then $g^{(1)}(k,\tau)$ shows a single relaxation, whose temporal evolution is determined by the probe self-diffusion coefficient.

Recently, Akcasu et al.[36] performed an equivalent analysis focused on ternary solutions of linear polymers. If only one polymer species scatters light, then if the scattering polymer is nondilute, two relaxational modes are, in general, predicted. However, if the scattering polymer is dilute, only one relaxational mode is predicted. Borsali et al.[37] report scattering studies on polystyrene/poly(dimethylsiloxane) solutions that quantitatively confirm Akcasu et al.'s[36] analysis, including in particular the transition from two to one visible modes as the scattering polymer is made dilute.

In the systems we studied, the probes dominate scattering and are highly dilute. The scattering spectrum that we studied here is therefore expected[34-36] to exhibit only one relaxation, corresponding to probe single-particle diffusion.

Probe Diffusion Measurements

This section treats systems in which cumulant expansions represent $S(k,t)$ adequately, D being inferred from K_1, namely, solutions of 60, 100, 300, and (dilute) 1 MDa HPC. The variance $V = (K_2/K_1^2)^{1/2}$ increased with increasing c and M. Spectra of concentrated ($c > 5$ g/L) 1 MDa HPC are highly nonexponential and fit cumulant expansions poorly, even for truncation order $N = 8$; these spectra are considered later.

Figure 3 presents D of the probes against matrix concentration. Over the observed concentration range, D falls 1–3 orders of magnitude. Solid lines are stretched exponentials (eq 2) from (i) a fit of data at all c and (ii) a fit limited to low-concentration ($c < c_M$) data. Dashed lines show fits of high-concentration ($c > c_m$) data to

$$D = \bar{D}c^{-x} \tag{8}$$

c_M and c_m were taken from Table III, so the same cut-off concentrations were used for all transport coefficients. Fitting coefficients from D appear in Table IV.

With 60 and 100 kDa HPC, stretched exponentials describe $D(c)$ well (root-mean-square fractional errors < 12%). Each data set may also be described well by a stretched exponential at $c < c_M$ and a power law at $c > c_m$; over $0 \le c \le c_M$, fits of eq 2 to $c < c_M$ and to all c are almost indistinguishable. Root-mean-square fractional errors in a power-law fit for $c > c_m$ and in a stretched exponential

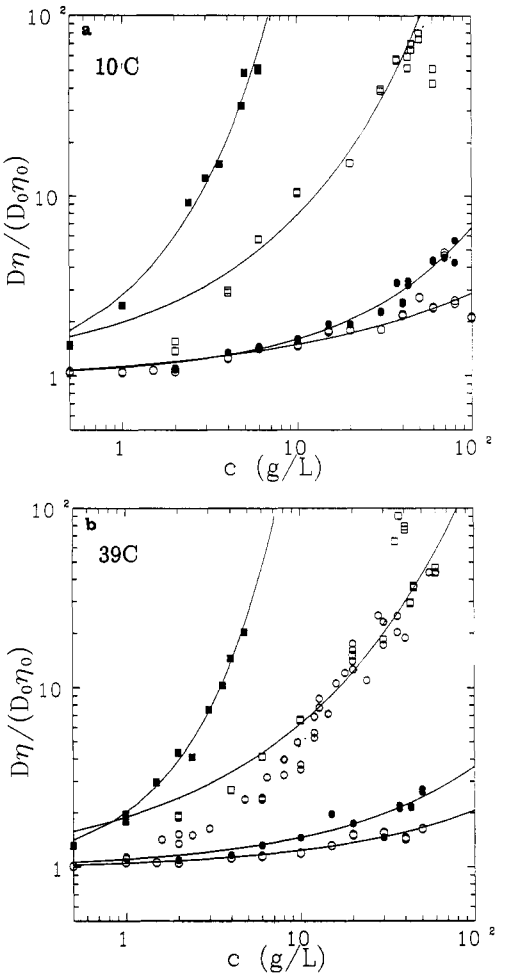

Figure 4. $D\eta/D_0\eta_0$ as a function of c for solutions of (○) 60 kDa, (●) 100 kDa, (□) 300 kDa, and (■) 1 MDa HPC at (a) 10 °C and (b) 39 and (upper set of open circles) 25 °C with 300 kDa HPC.

fit covering all c are nearly the same. $D(c)$ is described equally well by a single stretched exponential and by a stretched exponential/power-law composite. With 300 kDa HPC, at 10 and 25 °C a single stretched exponential and a stretched exponential/power-law combination fit equally well. At 39 °C a single stretched exponential fits poorly, the fitting error (19%) being markedly worse than errors (1 and 4%) for a composite stretched exponential/power law. At 39 °C, D in 300 kDa HPC shows the solutionlike–meltlike transition noted above for η. In 1 MDa HPC, cumulant expansions for $S(k,t)$ are only effective at $c < c_m$. In this regime, D decreases virtually exponentially in c.

Figure 4 tests the Stokes–Einstein equation, which predicts that $\kappa = D\eta/D_0\eta_0$ is independent of c. D_0 and η_0 refer to pure water. In a few cases, η was obtained by interpolation. If eq 1 were valid, $\kappa = 1$ would be obtained. We find that κ increases with c, perhaps by 2-fold in solutions of 60 and 100 kDa HPC and by far larger factors in relatively concentrated 300 kDa and 1 MDa HPC. Solid curves in Figure 4 are stretched exponentials, coefficients appearing in Table V. Except for a few outlier points, κ follows a stretched exponential accurately.

Alternative Spectral Analyses

As a second approach to interpreting $S(q,t)$, we systematically fit spectra to a Williams–Watts function[38]

$$g^{(1)}(q,t) = A_0 \exp(-\theta t^{\beta}) \tag{9}$$

previously[39] found to describe time correlation functions of some polymers approaching a glass. Here A_0 is an

Table V. Test of the Stokes–Einstein Equation: Fits of $\kappa = D\eta/D_0\eta_0$ to $\kappa = \kappa_0 \exp(\alpha c^\nu)$ with Constraint $\nu \geq 1/2$

M (kDa)	T	κ_0	α	ν	% rms
60	10	1.02	0.112	0.5	11.5
	39	0.97	0.077	0.50	4.4
100	10	0.98	0.126	0.59	8.5
	39	0.97	0.126	0.51	11.6
300	10	1.05	0.63	0.5	22
	39	1.12	0.52	0.5	17.3
1000	10	0.917	1.12	0.75	16
	39	0.94	0.75	0.92	7.8

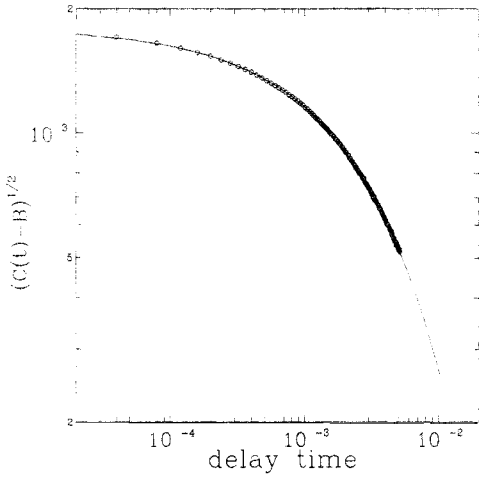

Figure 5. Field correlation function $(C(t) - B)^{1/2}$ for probes in 9 g/L of 1 MDa HPC at 39 °C and the Williams–Watts function (eq 9).

amplitude while θ and β are scaling coefficients. A representative fit appears in Figure 5. There is excellent agreement between $g^{(1)}(q,t)$ and the Williams–Watts form. We obtained θ and β as functions of c, M, and T. As discussed below, concentrated solutions of 1 MDa HPC show additional very slow decay modes.

Figure 6 plots θ against c. θ decreases strongly with increasing c, especially at larger M. θ was fit to $\theta = \theta_0 \exp(-ac^\nu)$, obtaining the solid lines and parameters given in Table VI. θ, like D, is described reasonably well by a stretched exponential. Figure 7 gives β against c. β is close to unity for probes in pure water and decreases with increasing c. Probes in 60 and 100 kDa HPC solutions show near-single-exponential spectra, β being in the range 0.85–1. At larger M and c, β decreases, to 0.7–0.8 in 300 kDa HPC at $c \geq 30$ g/L. Probes in 1 MDa HPC show β as small as 0.6–0.7, even for c as low as 10 g/L.

An alternative parametrization of the Williams–Watts form is

$$g^{(1)}(q,t) = A_0 \exp(-(t/\tau)^\beta) \qquad (10)$$

τ being an internal time scale. Equations 9 and 10 are equivalent under $\theta = \tau^{-\beta}$, so separate fits to eq 10 are unnecessary. Equation 10 has the attractive feature that τ has dimensions of time, t/τ being dimensionless, but forms like eq 9 also arise naturally. There is no obvious *a priori* reason to prefer θ or τ.

Figure 8 plots τ against c for all M and T. In pure water at 10 °C, τ is 0.55 ms. With increasing c, τ increases markedly, reaching nearly 1 s in 60 g/L of 300 kDa HPC. At fixed c, τ increases with increasing M. The time scale τ and scaling parameter θ do not have the same concentration dependences, but both are described well by stretching exponentials in c. Solid lines in Figure 8 correspond to parameters in Table VII.

Figure 6 tested the Stokes–Einstein equation against the D that describes the initial slope of $S(k,t)$. η has a far stronger concentration dependence than D. We made

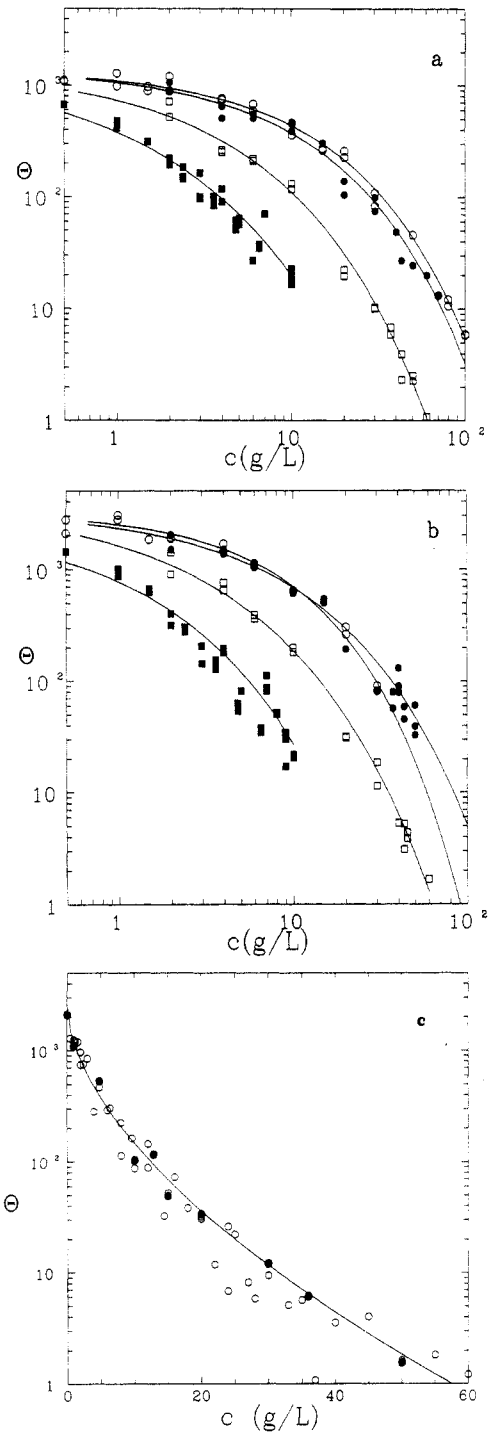

Figure 6. θ (units $s^{-\delta}$) from fits of eq 9 to spectra of (○) 60 kDa, (●) 100 kDa, (□) 300 kDa, and (■) 1 MDa HPC/H_2O at (a) 10, (b) 39, and (c) 25 °C (300 kDa HPC, single-τ (open circles) and multi-τ (filled circles) spectra). Solid lines are stretched exponentials.

(Figure 9) a similar comparison with τ, plotting $\tau\eta_0/\tau_0\eta$ against c. If $\tau \sim \eta^1$, simple horizontal lines would be seen. Especially at large M, $\tau\eta_0/\tau_0\eta$ declines with increasing c, values $\approx$0.01 being found. The time scale characterizing the body of our spectra is thus not determined by the solution viscosity.

The wave-vector dependence of $S(q,t)$ was examined for probes in 300 kDa and 1 MDa HPC. Scanning the scattering angle varied q^2 over a 6-fold range. For 300 kDa HPC, c included 0, 0.5, 5, 10, 30, and 40 g/L; for 1 MDa HPC, c included 0, 0.2, 5, 9, and 20 g/L. Plots of θ against q^2 reveal a linear relationship between these variables. Intercepts (the $q^2 \to 0$ limits of θ) are small and scattered randomly around zero. log–log plots of τ against

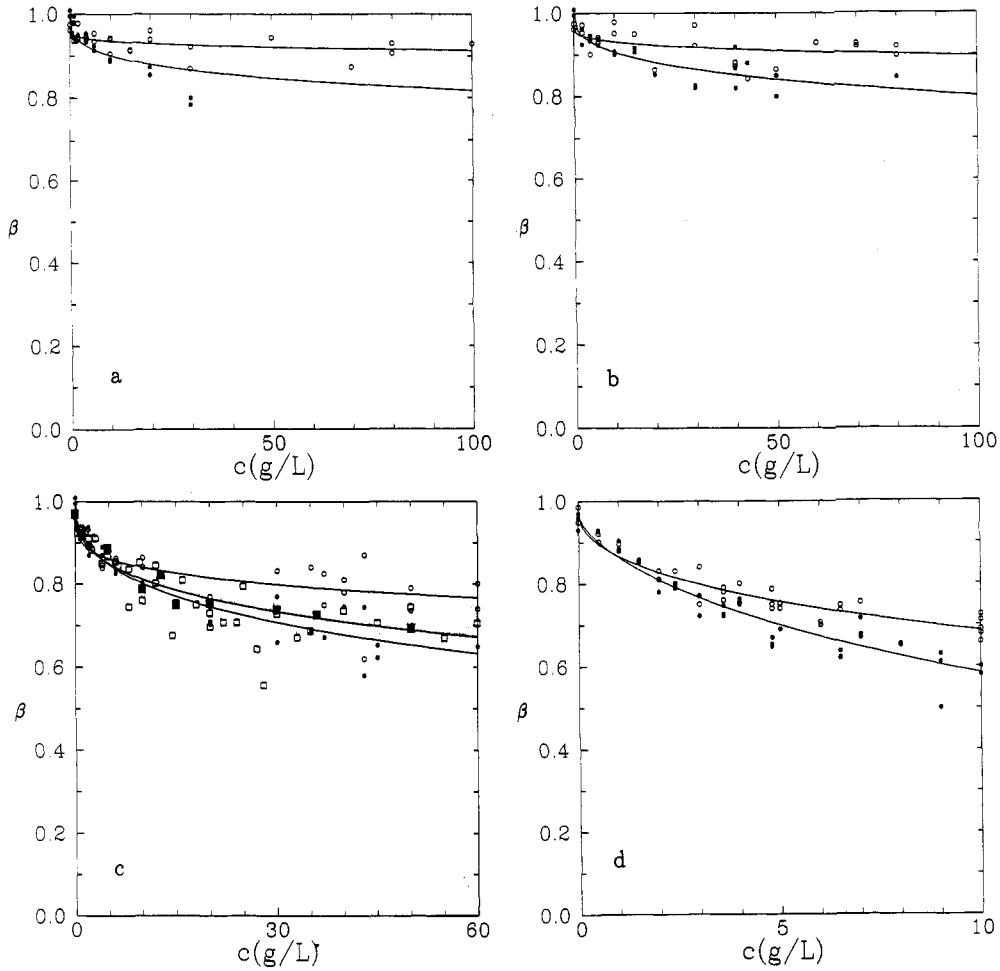

Figure 7. β from fits of eq 9 as a function of c at (○) 10, (□,■) 25, and (●) 39 °C for (a) 60 kDa, (b) 100 kDa, (c) 300 kDa, and (d) 1 MDa HPC. Lines are guides for th eye.

Table VI. Dependence of the Williams–Watts Function Parameter θ on c and M: Fits to $\theta = \theta_0 \exp(-\alpha c^{\nu})$

M (kDa)	T	θ_0	α	ν	% rms
60	10	1400	0.247	0.68	12.3
	39	3275	0.272	0.75	12.8
100	10	1420	0.297	0.66	18
	39	3450	0.398	0.61	25
300	10	1460	0.690	0.57	18
	25	2545	0.75	0.58	26
	39	3900	0.87	0.54	20
1000	10	1488	1.37	0.50	23
	39	2685	1.24	0.57	32

q^{-1} are also linear, with points being scattered randomly around the best-fit line. If one writes $\tau \sim q^{-2/\beta}$, the β determined from a $\tau - q^{-1}$ plot is within 3–10% of the average of the β parameters obtained from fits of spectra to the Williams–Watts function. $S(q,t)$ therefore shows the q^2 dependence expected for transport of a conserved quantity.

A third approach to analyzing spectra is to apply the method of moments, using

$$\frac{\int_0^\infty d\tau\, [S(q,\tau) - B]^{1/2}}{S(q,0)} = \langle 1/\Gamma \rangle \qquad (11)$$

to extract the average inverse relaxation rate. For an exponential spectrum $\langle \Gamma^{-1} \rangle^{-1}/q^2$ is the familiar diffusion coefficient. The Williams–Watts function gives

$$\int_0^\infty d\tau \exp(-(t/\tau)^{\beta}) = \tau \Gamma(\beta^{-1}) \qquad (12)$$

Here $\beta \in (0.5, 1)$, so the gamma function $\Gamma(\beta^{-1}) \in 0.85$–1, and the moments-method value for $\langle 1/\Gamma \rangle$ is always within 15% of τ^{-1}. For the spectra considered thusfar, replacing τ of Figures 8 and 9 with $\langle 1/\Gamma \rangle$ of eqs 11 and 12 would have only small quantitative consequences.

As a fourth alternative to cumulants, we fit spectra to sums of two-cumulant series, i.e.

$$[S(q,t) - B]^{1/2} = \exp\left(\sum_{j=0}^{2} \frac{K_{1j}(-t)^j}{j!}\right) + \exp\left(\sum_{j=0}^{2} \frac{K_{2j}(-t)^j}{j!}\right) \qquad (13)$$

Equation 13 corresponds to a distribution of decay times that is a sum of two Gaussians. The K_{1j} and K_{2j} were recovered via nonlinear least squares using simplex and Marquardt algorithms. Equation 13 is equivalent to the symmetric two-peak output sometimes seen from Laplace inversion programs; the number of independent parameters used here (six) is consistent with the number of independent parameters supported[31] by light scattering spectra having physically-plausible signal-to-noise ratios.

In solutions of 1 MDa HPC, the two-peak relaxation distribution worked adequately well for $c \leq 5$ g/L. At larger c, there were systematic deviations from eq 13. To a first approximation, a two-Gaussian relaxation distribution gives satisfactory results only when a conventional cumulants expansion is satisfactory. Difficulties with low-N cumulant fits in large-M samples are therefore not due to the presence of well-separated slow spectral modes.

Some of our results could be explained by the presence of a fast mode in our spectra. Using the narrowest channel widths (100 nS/channel) available from our correlators, we saw limited evidence of a weak, rapidly-decaying ($1/e$ time $\leq 10^{-3}\tau$), q-independent mode. With respect to the spectra analyzed above, this fast mode would have decayed

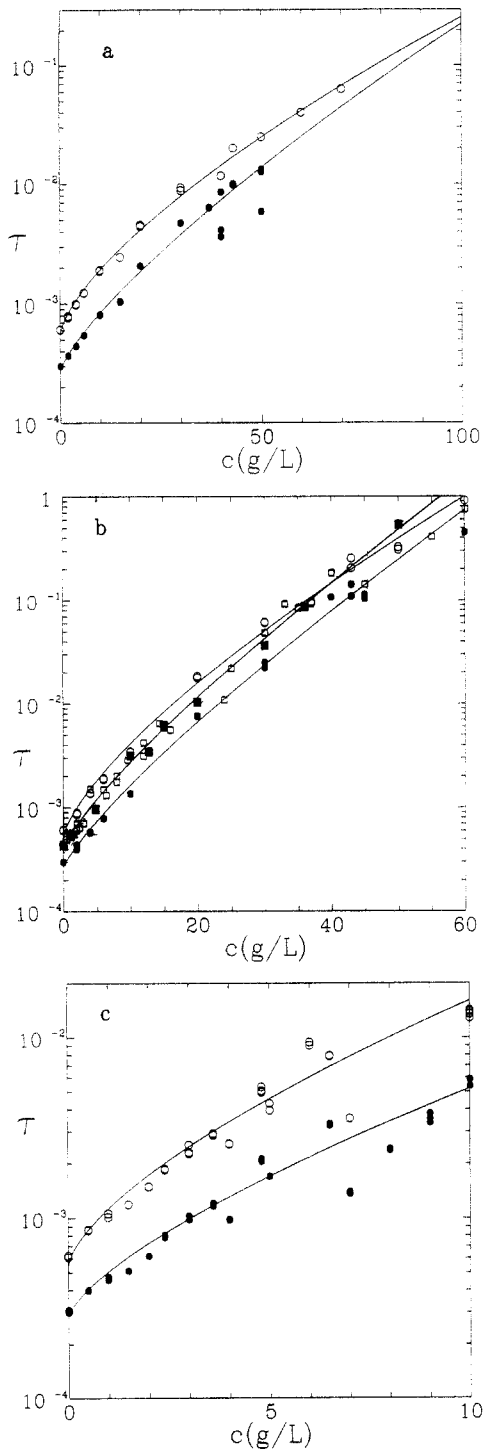

Figure 8. τ (s) of eq 10 against c at (○) 10, (□,■) 25, and (●) 39 °C for probes with (a) 100 kDa, (b) 300 kDa, and (c) 1 MDa HPC. Solid lines are stretched exponentials.

Table VII. Dependence of the Williams–Watts Function Parameter τ of Equation 10 on c and M: Fits to $\tau = \tau_0 \exp(ac^{\nu})$

M (kDa)	T	$\tau_0 \times 10^4$ (s)	a	ν	% rms
60	10	5.51	0.188	0.74	6.2
	39	2.98	0.081	1.00	5.0
100	10	5.58	0.25	0.70	9.7
	39	2.76	0.18	0.78	21
300	10	5.28	0.385	0.73	15
	25	3.91	0.28	0.83	18
	39	2.67	0.27	0.82	18
1000	10	5.46	0.72	0.67	20
	39	2.84	0.58	0.70	22

completely within the first two or three correlators channels, so it would not have affected our data analysis. Namely, for a Williams–Watts form, τ is determined by

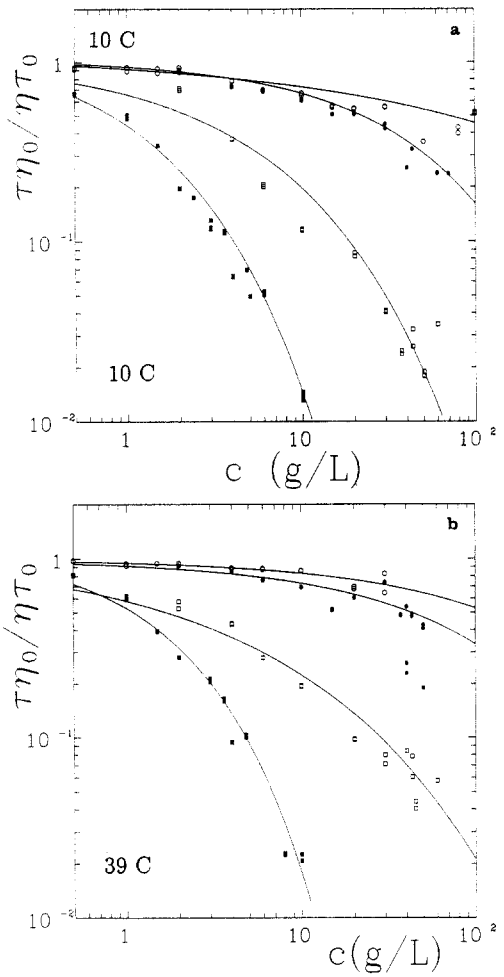

Figure 9. $\tau\eta_0/\tau_0\eta$ against polymer concentration c for solutions of (○) 60 kDa, (●) 100 kDa, (□) 300 kDa, and (■) 1 MDa hydroxypropylcellulose at (a) 10 and (b) 39 °C. Especially at large M, η increases with c much more rapidly than does the time scale τ of the Williams–Watts spectral representation.

the $1/e$ point of the field correlation function, namely, $\tau = t$ when $g^{(1)}(q,t) = 1/e$. A weak, very fast exponential mode has no effect on the $1/e$ time, because it affects neither $g^{(1)}(q,\tau)$ nor the extrapolation that obtains $g^{(1)}(q,0)$.

To reinforce the conclusion that an unrecognized fast mode did not perturb our results, we made a more detailed study of spectra of a range of 300 kDa and 1 MDa samples, with $0 \le c \le 50$ g/L at 300 kDa and $0 \le c \le 15$ g/L at 1 MDa. For each sample, multiple spectra were obtained, first with a 1-μs channel widths, and then with channel widths increasing roughly geometrically, e.g., 1, 3, 9, and 12 μs on consecutive spectra. Spectra cover a 10- to 100-fold decay of $g^{(1)}(q,t)$ and thus a 100- to 10 000-fold decay of $S(q,t)$.

To analyze these multi-τ spectra, for each sample all spectra were fit simultaneously to a Williams–Watts function, using the same (θ,β) for all spectra and an independent A_0 for each spectrum. Spectra with the largest channel widths disappear into the noise at large t; fitting was terminated modestly above the noise level. With the smallest channel widths, in some cases the base-line channels had a delay time sufficiently small that $g^{(1)}(q,\tau)$ had not decayed to zero at the base-line location. For these spectra, the "base-line", channels were used as additional data channels, with B for these spectra was used as a free parameter.

An exemplary spectrum appears as Figure 10; the Williams–Watts function works well even at times $\sim 10^{-4}\tau$, confirming that extremely rapid decays do not perturb

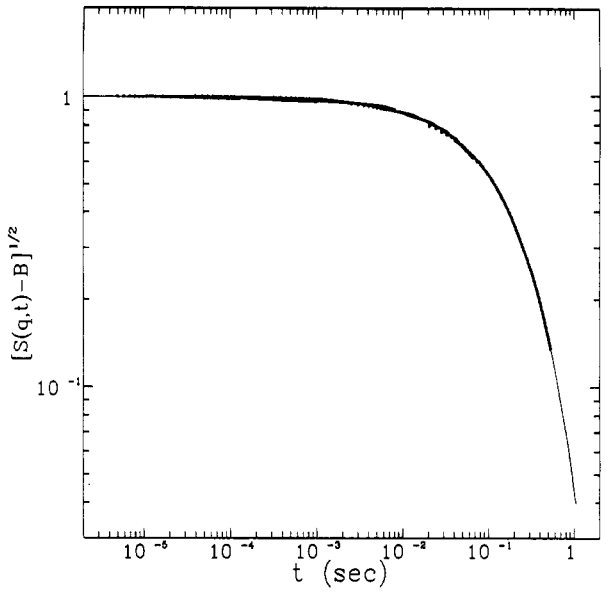

Figure 10. Merged spectra (using channel widths of 1, 8, 64, 510, and 4100 μs) of probes in 50 g/L of 300 kDa HPC, showing that a Williams–Watts expansion works well even for times $t \sim 10^{-4}\tau$.

our estimates of θ. However, in 1 MDa HPC at $c \geq 25$ g/L the fitting process fails, because (for $t \geq 1$ s) spectra change from a Williams–Watts to an apparent power-law decay. There thus appears to be an upper c-M boundary to the validity of our results. This paper analyzes data in which long-time power-law decays were not seen.

Discussion

Probe diffusion in HPC/water has previously been studied by Brown and Rymden,[13] Yang and Jamieson,[12] Russo et al.,[15,16] and this laboratory.[17] Brown and Rymden studied 8×10^5 Da HPC at fixed T for $c \leq 2$ g/L, obtaining viscosities as large as 7 cP. They report non-Stokes–Einsteinian behavior, with $D\eta/D_0\eta_0 \approx 4$ in 2 g/L of HPC.

Russo et al.[15] using 907-Å-radius probes in the same 1 MDa HPC (same supplier, same lot number) that we used, at concentrations $c \leq 1.5$ g/L. They also studied 794- and 1814-Å spheres in 300 kDa HPC/TX-100 for $c \leq 10$ g/L. Reference 15 used primarily data analysis based on Laplace inversion, finding that spectra were usefully characterized by a sum of exponentials, the implied distribution of diffusion coefficients having a bi- or trimodal form. The dominant relaxation was a slow mode, but a faster (by perhaps 3-fold), weaker mode was also present. Russo et al. emphasize D from a dominant slow mode, comparing this D with η. They found only a weak failure of eq 1, $D\eta$ increasing perhaps 2-fold between 0 and 1.5 g/L.

Yang and Jamieson[12] studied HPC/Triton X-100/water systems for a range of sphere sizes and HPC molar masses (1×10^5–8.5×10^5 Da), albeit only at concentrations ($c <$ 8–40 g/L) and viscosities ($\eta_r < 50$) substantially smaller than the largest (100 g/L, 10^6 cP) reached here. Yang and Jamieson remained in regions where $D/D_0 > 0.2$. For 100 and 140 kDa HPC, $D\eta/D_0\eta_0$ remained close to unity at elevated c. In Yang and Jamieson's solutions of the 450 and 850 kDa polymers, failures of eq 1 were more conspicuous, $D\eta/D_0\eta_0 \approx 5$ being attained; the failure was larger for smaller probes.

Russo et al.[15] emphasize differences between their measurements and Brown et al.'s.[13] These disagreements appear to arise during the reduction of $S(q,t)$ to D. Russo et al. and Brown et al. both found (as did we) that probe spectra become increasingly nonexponential with increasing c and M. Brown et al. used cumulants analysis, which (when properly converged) reports an intensity-weighted average of all relaxations.' Russo et al. decomposed spectra into a distribution of exponentials and used only the slow mode to compute D, saying[15] of the fast mode "the uniquely correct interpretation of the fast mode is not as clear as the fact that it can substantially corrupt data interpretation if it is not properly accounted for".

The effect of removing fast modes is clear. Russo et al.[15] systematically excluded a fast mode, so Russo et al. obtained a smaller D than did Brown et al.[13] under nearly the same conditions. Since D is too large relative to η, Russo et al. found a smaller failure of eq 1 than did Brown et al. Russo et al. note that the fast mode, in some cases, has a larger decay rate than their probes would have in pure solvent and conclude that the fast mode therefore cannot be simple probe diffusion. However, D of polystyrene sphere probes in some poly(ethylene oxide)/water solutions is substantially larger than D of the same probes in pure water.[22] In the poly(ethylene oxide) system, there is no slow mode, so the rapid decay must correspond to sphere diffusion. Until the line shape is given a complete physical interpretation, it is difficult to decide between Russo et al.'s or Brown et al.'s calculations of D from $S(q,\tau)$.

Relative to previous work,[12–17] our experiments cover a significantly wider range of c, M, and T. For systems of the largest M, Brown et al.[13] and Russo et al.[15] worked at $c < 2$ g/L; i.e., they only covered $c < c_M$. Data of Russo et al.[16] on 300 kDa HPC and of Yang et al.[12] on a series of HPC samples are also limited to $c \leq c_M$. Our measurements of D and η are consistent with these literature results for $c \leq c_M$. However, our results extend to the meltlike ($c \geq c_m$) regime, i.e., to larger η and smaller D/D_0 than most previous studies. For $M \approx 1 \times 10^6$, we find that η goes over to c^x behavior only above 2 g/L; only above a few grams per liter does one observe $D\eta/D_0\eta_0 \gg 1$. Previous work[13–16] was limited to lower concentrations and would not have observed the dramatic failures of eq 1 that we report.

We[17] had previously reported D but not η of probes in 60 kDa HPC at 10 and 40 °C, finding results quantitatively consistent our new data. For the concentration dependence of D, at 10 °C we find $(\alpha, \nu) = (0.20, 0.72)$, while our previous work on this material found (0.175, 0.74). The difference in (α, ν) represents the operational experimental error. On increasing T to 39 °C, we find $\alpha = 0.1$ and $\nu = 0.9$; at 40.5 °C Phillies and Clomenil[17] report $\alpha = 0.06$ and $\nu = 1.1$ (or $\alpha = 0.092$ with $\nu = 1$ forced). With increasing T, α decreases and ν increases.

Previous studies[21–24] on the temperature dependence of probe diffusion in other polymers found that D tracks accurately $\eta(T)$ of the solvent, with no indication of glass temperature effects. In these systems, water as a good solvent at all temperatures, so no significant effect of T on polymer conformation was expected. In contrast, HPC/water has a pseudo-Θ transition near 41 °C. As discussed previously,[17] as one approaches the Θ point, reptation-based[1] and hydrodynamic scaling[7] pictures of polymer dynamics both predict $\nu < 1$ under good conditions and $\nu \approx 1.0$ under Θ-like conditions. Indeed, with 60 kDa HPC $\nu = 0.75$ at 10 °C, while between 39 and 40.5 °C ν increases from 0.90 toward 1.0. Both reptation and hydrodynamic scaling models predict[17] that α falls as the Θ temperature is approached; for the 60 kDa sample, at 10, 39, and 40.5 °C one finds α falling from 0.20 to 0.10 to 0.06.

The effect of T on D is marked for 60 kDa HPC but diminishes substantially with increasing M. From Table IV, with the 100 and 300 kDa polymers ν increases with increasing T while α falls, but the variations with T in ν and α decline with increasing M. In solutions of 1 MDa HPC, α is nearly independent of T; the small concentration

range covered with the 1 MDa polymer makes it difficult to determine ν with great precision.

Probes in HPC/water have nonexponential spectra, the deviations from exponentiality increasing with increasing c and M.[13,16] Russo et al.[15] decomposed spectra into bimodal distributions of exponentials, interpreting the slower mode as self-diffusion. Seeming bimodal relaxation patterns are also seen in aqueous solutions of nonneutralized 1 MDa[23] and 750 kDa (but not 450 kDa) poly(acrylic acid), in which optical probe spectra assume a bimodal form. Here we find that our nonexponential spectra are described well by a single Williams–Watts function,[38] which is a stretched exponential in time.

The Williams–Watts function also describes well spectra of polymer systems near a glass transition.[39] Systems here are far from the glass transition but nonetheless have a Williams–Watts form. Ngai and collaborators[40] have introduced general arguments in the form of a coupling model, suggesting that stretched exponential dependences on concentration and time are not independent phenomena and should be expected to occur simultaneously, as was observed here.

Summary

We studied shear viscosity and optical probe diffusion in HPC/water solutions. The shear viscosity shows a stretched-exponential concentration dependence at lower c and a power-law concentration dependence at larger c. Such a transition was found previously in reanalyses[28] of literature results on some but not all concentrated, large-M, polymer solutions, where it appears to mark the transition between solutionlike and meltlike behavior. In most cases the concentration dependence of D is consistent with a stretched- exponential at all c, including concentration regimes where $\eta \sim c^x$. Our data are also consistent with stretched-exponential behavior at low c and c^x behavior at elevated c. The temperature dependence of the exponential parameters α and ν is strong for 60 kDa HPC but much weaker for systems having larger M.

Comparison of D and η with the Stokes–Einstein equation finds that eq 1 fails at large c and M. Probe particles diffuse faster than expected from η, $D\eta/D_0\eta_0 \approx 100$ being observed in some cases. $D\eta/D_0\eta_0$ is consistently larger at 10 °C (good solvent) than at 39 °C (near-pseudo-Θ).

Probe spectra become increasingly nonexponential as c and M are increased. The Williams–Watts function (eqs 9 and 10) fits solution spectra very well. While this form has previously been applied to correlation functions of glassy systems,[39,40] we are not aware of a successful application to polymer solutions.

Quantitatively, the Williams–Watts stretching parameter δ decreases from near 1.0 for probes in pure water to $\approx$0.6 at large c and M. Over the same range of c and M the time constant τ increases by up to 3 orders of magnitude. τ, like D, has a stretched-exponential dependence on c. $\tau\eta_0/\tau_0\eta$ is closely similar to $D_0\eta_0/D\eta$, relaxation times being up to 2 orders of magnitude smaller than expected if τ were determined by the macroscopic η. $\tau\eta_0/\tau_0\eta$ is consistently closer to 1.0 under near-Θ conditions (39 °C) than under good solvent conditions (10 °C).

Acknowledgment. We thank Dr. Rajesh Beri, Ms. Cynthia Sullivan, and Professor James E. Rollings, Department of Chemical Engineering, Worcester Polytechnic Institute, for the polymer molecular weight analyses.

References and Notes

(1) de Gennes, P.-G. *Scaling Concepts in Polymer Physics*; Cornell University Press: Ithaca, NY, 1979.

(2) Doi, M.; Edwards, S. F. *The Theory of Polymer Dynamics*; Clarendon Press: Cambridge, U.K., 1986.

(3) Hess, W. *Macromolecules* **1986**, *19*, 1395; **1987**, *20*, 2587.

(4) Skolnick, J.; Yaris, R. *J. Chem. Phys.* **1987**, *88*, 1407, 1418.

(5) Oono, Y.; Baldwin, P. R. *Phys. Rev. A* **1986**, *33*, 3391.

(6) Ngai, K. L.; Rendell, R. N.; Rajagopal, S. T. *Ann. N.Y. Acad. Sci.* **1984**, *484*, 150.

(7) Phillies, G. D. J. *J. Phys. Chem.* **1989**, *93*, 5029.

(8) Phillies, G. D. J. *Macromolecules* **1987**, *20*, 558.

(9) Phillies, G. D. J. *Macromolecules* **1986**, *19*, 2367.

(10) Lodge, T. P.; Rotstein, N. A.; Prager, S. *Adv. Chem. Phys.* **1990**, *79*, 1.

(11) Skolnick, J.; Kolinski, A. *Adv. Chem. Phys.* **1989**, *78*, 1.

(12) Yang, T.; Jamieson, A. M. *J. Colloid Interface Sci.* **1988**, *126*, 220.

(13) Brown, W.; Rymden, R. *Macromolecules* **1986**, *19*, 2942.

(14) Mustafa, M.; Tipton, D. L.; Barkley, M. D.; Russo, P. S.; Blum, F. D. *Macromolecules* **1993**, *26*, 370.

(15) Mustafa, M.; Russo, P. S. *J. Colloid Interface Sci.* **1989**, *129*, 240.

(16) Russo, P. S.; Mustafa, M.; Cao, T.; Stephen, L. K. *J. Colloid Interface Sci.* **1988**, *122*, 120.

(17) Phillies, G. D. J.; Clomenil, D. *Macromolecules* **1993**, *26*, 167.

(18) Phillies, G. D. J.; Ullmann, G. S.; Ullmann, K.; Lin, T.-H. *J. Chem. Phys.* **1985**, *82*, 5242.

(19) Turner, D. N.; Hallet, F. R. *Biochim. Biophys. Acta* **1976**, *451*, 305.

(20) Laurent, T. C.; Pietruskiewicz, A. *Biochim. Biophys. Acta* **1961**, *49*, 258.

(21) (a) Phillies, G. D. J.; Gong, J.; Li, L.; Rau, A.; Zhang, K.; Yu, L.-P.; Rollings, J. *J. Phys. Chem.* **1989**, *93*, 6219. (b) Phillies, G. D. J.; Quinlan, C. A. *Macromolecules* **1992**, *25*, 3310.

(22) (a) Ullmann, G. S.; Ullmann, K.; Lindner, R. M.; Phillies, G. D. J. *J. Phys. Chem.* **1985**, *89*, 692. (b) Ullmann, G. S.; Phillies, G. D. J. *Macromolecules* **1983**, *16*, 1947.

(23) Lin, T.-H.; Phillies, G. D. J. *J. Colloid Interface Sci.* **1984**, *100*, 82.

(24) (a) Phillies, G. D. J.; Malone, C.; Ullmann, K.; Ullmann, G. S.; Rollings, J.; Yu, L.-P. *Macromolecules* **1987**, *20*, 2280. (b) Phillies, G. D. J.; Pirnat, T.; Kiss, M.; Teasdale, N.; Maclung, D.; Inglefield, H.; Malone, C.; Yu, L.-P.; Rollings, J. *Macromolecules* **1989**, *22*, 4068. (c) Phillies, G. D. J.; Rostcheck, D.; Ahmed, S. *Macromolecules* **1992**, *25*, 3689.

(25) Langevin, D.; Rondelez, F. *Polymer* **1978**, *19*, 875.

(26) Phillies, G. D. J.; Peczak, P. *Macromolecules* **1988**, *21*, 214.

(27) Pearson, D. S. *Rubber Chem. Technol.* **1987**, *60*, 439.

(28) Phillies, G. D. J. *J. Phys. Chem.* **1992**, *96*, 10061.

(29) Enomoto, H.; Einaga, Y.; Teramoto, A. *Macromolecules* **1985**, *18*, 2695.

(30) Koppel, D. E. *J. Chem. Phys.* **1972**, *57*, 4814.

(31) Phillies, G. D. J. *J. Chem. Phys.* **1988**, *89*, 91.

(32) Corona, A.; Rollings, J. E. *Sep. Sci. Technol.* **1988**, *23*, 855. Callec, G.; Anderson, A. W.; Tsao, G. T.; Rollings, J. E. *J. Appl. Polym. Technol.* **1984**, *22*, 287.

(33) Phillies, G. D. J.; Stott, J.; Ren, S. Z. *J. Phys. Chem.*, in press.

(34) Phillies, G. D. J. *J. Chem. Phys.* **1974**, *60*, 983.

(35) Jones, R. B. *Physica* **1979**, *97A*, 113.

(36) Akcasu, Z.; Benmouna, M.; Benoit, H. *Polymer* **1986**, *27*, 1935.

(37) Borsali, R.; Duval, M.; Benmouna, M. *Macromolecules* **1989**, *22*, 816.

(38) Williams, G.; Watts, D. C. *Trans. Faraday Soc.* **1970**, *66*, 80.

(39) Patterson, G. D. In *Relaxations in Complex Systems*; Ngai, K. L., Wright, G. B., Eds.; National Technical Information Service: Washington, DC, 1984; p 111.

(40) (a) Ngai, K. L.; Rendell, R. W.; Rajagopal, A. K.; Teitler, S. *Ann. N.Y. Acad. Sci.* **1986**, *484*, 150. (b) McKenna, G. B.; Ngai, K. L.; Plazek, D. J. *Polymer* **1985**, *26*, 1651. (c) Rendell, R. W.; Ngai, K. L.; McKenna, G. B. *Macromolecules* **1987**, *20*, 2250.